

LSTM-COX Model: A Concise and Efficient Deep Learning Approach for Handling Recurrent Events

Run-Quan Zhang^a, Xiao-Ping Shi^{b,*}

^a*XinJiang University, Urumqi 830046, China*

^b*XinJiang University, Urumqi 830046, China*

Abstract

In the current field of clinical medicine, traditional methods for analyzing recurrent events have limitations when dealing with complex time-dependent data. This study combines Long Short-Term Memory networks (LSTM) with the Cox model to enhance the model's performance in analyzing recurrent events with dynamic temporal information. Compared to classical models, the LSTM-Cox model significantly improves the accuracy of extracting clinical risk features and exhibits lower Akaike Information Criterion (AIC) values, while maintaining good performance on simulated datasets. In an empirical analysis of bladder cancer recurrence data, the model successfully reduced the mean squared error during the training phase and achieved a Concordance index of up to 0.90 on the test set. Furthermore, the model effectively distinguished between high and low-risk patient groups, and the identified recurrence risk features such as the number of tumor recurrences and maximum size were consistent with other research and clinical trial results. This study not only provides a straightforward and efficient method for analyzing recurrent data and extracting features but also offers a convenient pathway for integrating deep learning techniques into clinical risk prediction systems.

Keywords:

LSTM, Recurrence, Survival

1. Introduction

In clinical medicine, recurrent events have profound implications for disease management and patient survival outcomes, necessitating precise prediction and analysis for cancer treatment, chronic disease management, and postoperative recovery. The inherent temporal characteristics of these events—such as intervals and frequency—provide crucial predictive information about the natural progression of diseases and the effectiveness of treatments. Classical methods, such as the Cox proportional hazards model[1] and the Anderson-Gill model[2], have achieved significant milestones in survival data and recurrent event data analysis. However, the efficacy of existing models is challenged by the time-dependence and high-dimensional features of clinical recurrence data. To effectively address these issues, we need to develop risk prediction models capable of more accurately predicting and analyzing the dynamic information of disease recurrence.

In the field of survival analysis, deep learning techniques based on models like DeepSurv[3] and RNN-SURV[4] have enhanced neural networks' ability to handle nonlinear associations and censored data, thereby improving the accuracy and efficiency of survival analysis. Additionally, researchers have proposed a new deep learning framework[5] for survival analysis of recurrent events with multiple competing risks. This

framework employs LSTM networks to enhance the prediction capabilities regarding event timing and causes.

This study focuses on bladder cancer—a field with a high recurrence rate and rapid disease progression—using related datasets for in-depth analysis. Studies have shown that factors such as the number of tumors and static tumor shapes are closely related to early recurrence of bladder cancer[6], emphasizing the importance of complete transurethral resection of bladder tumors in reducing such risks[7]. Meanwhile, emerging research on the prognostic utility of extracting nuclear features through machine learning reveals the potential of machine learning techniques in predicting non-muscle invasive bladder cancer recurrence[8], enriching the discussion on deep learning applications in this field[9][10].

In the field of survival analysis research, the combination of deep learning models and traditional statistical methods brings potential for improved prediction accuracy. This study explores a novel approach that combines Long Short-Term Memory networks (LSTM) with the Cox model to handle time-sensitive clinical recurrence data. Through this integration, this study aims to leverage the capabilities of LSTM[11] to enhance the processing of dynamic and static variables[12][13], thereby improving the accuracy of risk prediction models. By more effectively learning temporal information, this approach is expected to provide more robust support for clinical risk prediction. This integrated method not only supplements traditional models but also offers more accurate and comprehensive insights into the problem of disease recurrence.

*Corresponding author

Email addresses: 107552203540@stu.xju.edu.cn (Run-Quan Zhang), shixiaoping@xju.edu.cn (Xiao-Ping Shi)

2. Methods and Materials

2.1. Variable Definitions

Before delving into the methods and materials used in this study, we first summarize the key variables involved in the subsequent sections. The purpose of this is to ensure that readers can accurately understand the terminology and symbols used in data processing, model assumptions, and the analysis process, thereby better grasping these methods and their implementation details.

2.2. Dataset Description

This study employs the bladder cancer recurrence dataset, which is a publicly accessible resource on the Kaggle platform (<https://www.kaggle.com/datasets/utkarshx27/bladder-cancer-recurrences>). This dataset provides detailed information on 118 patients, including various recurrence events that occurred during their treatment. It comprehensively records multiple key attributes for each patient, such as the type of treatment administered (including placebo, vitamin B6, and thiotepa), the initial number of tumors, the maximum tumor size, recurrence frequency, the start and end time of each recurrence event, reasons for data truncation, tumor indicators during recurrence intervals, and event observation codes. The reasons for data truncation are categorized as follows: 0 indicates no recurrence (or censored), 1 indicates cancer recurrence, 2 indicates death due to bladder cancer, and 3 corresponds to death due to other or uncertain causes.

This dataset provides detailed time series data related to patient recurrences, offering a rich resource for analyzing bladder cancer recurrence patterns. In this study, the complete data of all 118 patients were selected, considering all recorded recurrence events to comprehensively evaluate the proposed LSTM and Cox model combination method. In Table 2, this study provides a descriptive statistical summary of the bladder cancer recurrence dataset, including minimum, median, mean, and maximum values. For example, the average number of tumors (Number) is 2.374, indicating the average number of tumors at the initial diagnosis. The maximum number of recurrences (Recur) is 9, showing that the patient with the highest recurrence frequency experienced 9 recurrences. Additionally, the table lists the frequency of different treatment types. Among them, patients treated with a placebo (Placebo) have the highest number of records, totaling 48. The choice of treatment type may affect recurrence rates and treatment efficacy, making this information potentially significant for analyzing treatment effects. This statistical information not only reflects the clinical characteristics of the dataset but also may indicate the long-term effects of treatments and patient survival outcomes. These statistics provide a foundation for our subsequent analysis of bladder cancer recurrence patterns and the evaluation of the effectiveness of different treatment methods, while also highlighting the complexity of the dataset and the challenges of the research.

2.3. Data Preprocessing

Data preprocessing involves removing non-essential columns, such as automatically generated indexes, and converting specific categorical variables into numerical formats. For example, in the `treatment` column, treatment methods are numerically encoded as: placebo (1), thiotepa (2), and vitamin B6 (3). Dots in the `rtumor` and `rsize` columns are replaced with NaNs, followed by appropriate handling of missing values. For cases with no recurrence or death, NaNs in the relevant columns are replaced with 0. Numerical features are standardized to reduce the impact of different magnitudes.

To meet the LSTM model's requirements for time series data, patient records are reorganized into fixed-length sequences. This process generates a three-dimensional array $D \in \mathbb{R}^{N \times T \times F}$. The sequence length is set to 3, and selected features include treatment type, number of tumors, size, and recurrence counts. These sequences are then converted into NumPy arrays and saved as `.npy` files for subsequent analysis.

2.4. Model assumptions and derivation

The LSTM-Cox model is built based on the following assumptions:

- Assumption 1: The LSTM network can capture and learn the complex nonlinear relationships between covariates X and time dependency. This is attributed to the LSTM's gating mechanisms (input gate, forget gate, and output gate) and state update functions, which effectively handle and remember long-term dependencies.

According to the research by Siegelmann and Sontag, RNNs can compute any computable function, similar to a Turing machine. LSTMs improve performance by overcoming the inherent gradient vanishing and exploding problems in RNNs, especially when handling long-term dependencies. For any complex time-varying function $f(X, t)$, there exists an LSTM architecture Θ_{LSTM} such that:

$$\lim_{\|\Theta_{LSTM}\| \rightarrow \infty} \|f(X, t) - \hat{f}_{\Theta_{LSTM}}(X, t)\| = 0, \quad (1)$$

where $\hat{f}_{\Theta_{LSTM}}(X, t)$ is the approximation of $f(X, t)$ by the LSTM, and $\|\Theta_{LSTM}\|$ denotes the complexity or size of the LSTM model.

- Assumption 2: The Cox model is semi-parametric, which means we can model the complex relationship between the features extracted by the LSTM network and recurrence data without making specific assumptions about the baseline hazard function $h_0(t)$. The classical Cox model fails to capture the underlying time-varying effects of covariates, which can be demonstrated using the Weibull parametric survival model.

Let the true hazard function be $h^*(t|X)$, and the hazard function estimated by the LSTM-Cox model be $\hat{h}(t|X)$. The objective of using the LSTM-Cox model is to minimize the prediction error $E \left[\left(\hat{h}(t|X) - h^*(t|X) \right)^2 \right]$, to approximate the true hazard function as closely as possible.

Table 1: Summary of Key Variables Used in the Study

Variable Type	Variable Name	Variable Symbol	Definition
Input Variables	Covariates Matrix	X	Matrix containing feature data for all patients, used as input to the models.
	Time-step Features	X_t	Features at time step t , used in LSTM model calculations.
Output Variables	LSTM Output	$\hat{f}_{\Theta_{LSTM}}(X, t)$	The output from the LSTM model approximating function $f(X, t)$.
	Hazard Function Estimate	$\hat{h}(t X)$	Estimated hazard function from the LSTM-Cox model.
Parameter Variables	LSTM Parameters	Θ_{LSTM}	Parameters defining the LSTM network structure and weights.
	Cox Model Coefficients	β	Regression coefficients of the Cox proportional hazards model.
Intermediate Variables	Hidden State at Time t	H_t	Hidden state of LSTM at time step t , used in further calculations.
Configuration Variables	Number of Samples	N	Total number of patient records analyzed.
	Number of Features	F	Total number of features considered after data restructuring.
	Number of Time Steps	T	Total number of time steps in the LSTM model.

Since the LSTM network can capture complex time series features and dynamic dependencies, theoretically, this model surpasses traditional survival analysis models in approximating complex nonlinear time-varying risk functions. Therefore, we can infer:

$$|Bias(\hat{h}_{LSTM-Cox}(t|X))| < |Bias(\hat{h}_{classicmodel}(t|X))| \quad (2)$$

Although integrating LSTM into the Cox model increases the model's complexity, through regularization and model selection processes (e.g., using dropout in LSTM), we can control the increase in variance, thereby ensuring that the overall prediction error remains at a low level. The design of the LSTM-Cox model maintains a balance between bias and variance, optimizing the overall prediction error.

Before delving into the specifics of the LSTM model design, Figure 1 provides a comprehensive overview of the LSTM-Cox model architecture, illustrating the process from data preprocessing to feature extraction for risk function estimation.

2.5. Model design and feature examination

2.5.1. LSTM model settings

In this study, we constructed the LSTM model using TensorFlow. First, the input layer of the model receives the preprocessed time series data. This input can be represented as the function

$$f : \mathbb{R}^{T \times F} \rightarrow \mathbb{R}^M$$

Table 2: Descriptive Statistics and Treatment Frequency of the Bladder Cancer Dataset

Statistic	Min	Median	Mean	Max
Number	1	2	2.374	8
Size	1	1	1.993	8
Recur	0	3	3.595	9
Start	0	4	11.2	52
Stop	0	23	23.8	64
Rtumor	1	2	3.07	8
Rsize	1	1	1.265	8
Enum	1	2	2.704	10
Category	Frequency			
Placebo	48			
Pyridoxine	32			
Thiotepa	38			

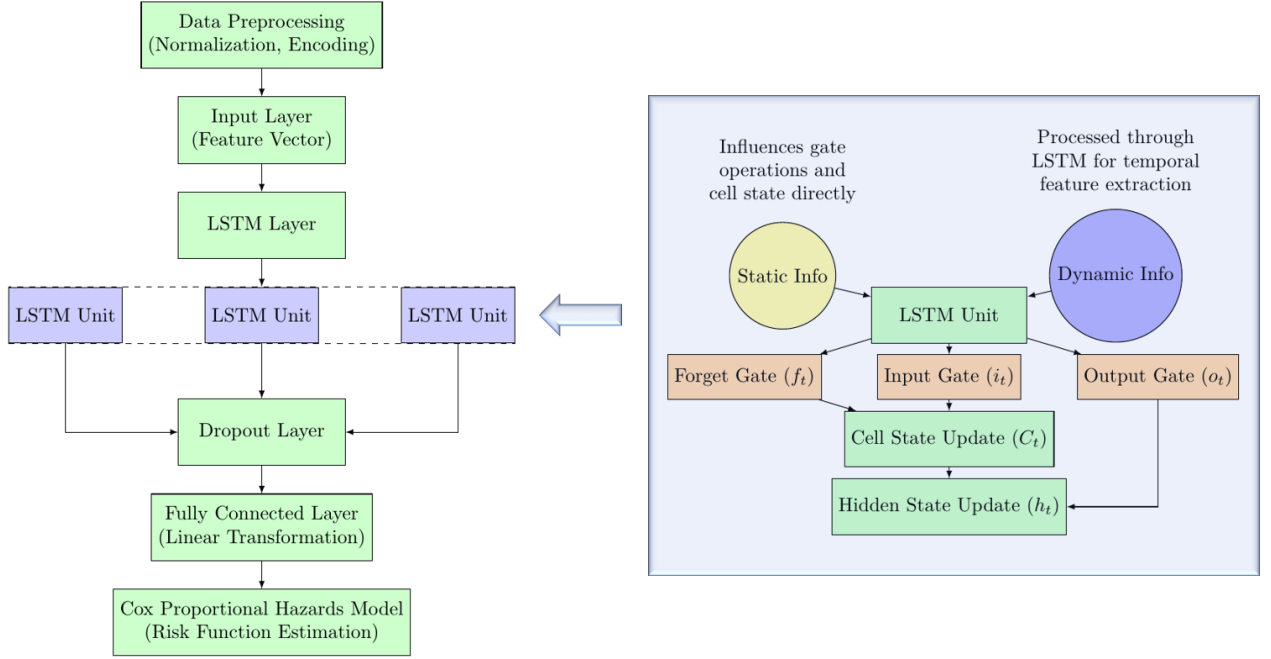


Figure 1: Overview of the LSTM-Cox model architecture. This figure depicts the sequential flow from data preprocessing, including normalization and encoding, through the LSTM layer with dropout regularization, and culminating in the fully connected layer feeding into the Cox Proportional Hazards Model for risk estimation.

where M represents the number of output features. The model includes a 20-unit LSTM layer set to return sequences at each time point

$$H = [h_1, h_2, \dots, h_T]$$

where each $h_t \in \mathbb{R}^U$ represents the hidden state at time step t , and U is the number of LSTM units. The updates of the LSTM can be computed using the following formula

$$H_t = \text{LSTM}(H_{t-1}, X_t)$$

where X_t is the input at the current time step and H_{t-1} is the hidden state of the previous time step. Additionally, to reduce overfitting, a Dropout layer is added, which randomly drops neurons using the formula

$$Y = \text{Dropout}(H, p)$$

where p is set to 0.5. The final layer of the model is a fully connected layer without an activation function to suit the subsequent Cox model.

To quantify the discrepancy between the model predictions and the actual results, mean squared error (MSE) is used as the loss function[14], mathematically expressed as

$$L(Y, \hat{Y}) = \frac{1}{N} \sum_{i=1}^N (Y_i - \hat{Y}_i)^2$$

where N is the sample size. This loss function is used by the model to measure the gap between the predicted values \hat{Y}_i and

the true values Y_i . The model parameters are adjusted to minimize the loss function, and optimization is performed using the Adam optimizer.

During the training phase, the model parameters θ are updated according to the principle of gradient descent to minimize the loss function[15]. The parameter update is performed as follows

$$\theta_{\text{new}} = \theta_{\text{old}} - \alpha \cdot \nabla_{\theta} L(Y, f(X; \theta))$$

where α is the learning rate, and ∇_{θ} denotes the gradient of the loss function with respect to θ . The model iterates for 100 epochs on the training dataset, with a batch size of 32, and its performance is evaluated on the validation set to monitor and prevent overfitting. After initial training, the model is evaluated on the test set, and its loss is calculated. Further performance optimization involves hyperparameter tuning, including changing the number of LSTM units, dropout ratio, and optimizer learning rate. Finally, time series features are extracted from the model to construct the Cox proportional hazards model.

2.5.2. Construction and Training of the Cox Proportional Hazards Model

The Cox proportional hazards model, initially proposed by Cox (1972), is a well-established method in survival analysis. This model assumes that an individual's hazard function $h(t)$ is the product of a baseline hazard function $h_0(t)$ and an exponential function of the covariates $\exp(\beta^T X)$, where β are the co-

efficients and X represents the covariates associated with each individual.

In this study, we extend the traditional Cox model to include features extracted from the LSTM network. The construction and training of the model begin with calculating the survival time T_i , obtained by computing the difference between the last observation end time (stop) and the first start time (start) for each patient. Additionally, to obtain the survival status δ_i , we check the survival status at the last time point in each patient's time series data and convert it into a binary variable.

The LSTM model processes the time-dependent covariates, generating a feature vector

$$F_{vec} = f(X; \theta)$$

where θ represents the parameters of the LSTM, and X represents the input data. These features, along with survival times and survival statuses, are compiled into a Pandas DataFrame.

Subsequently, the Cox model is trained using the CoxPHFitter from the lifelines library, with the hazard function now defined as:

$$h(t|F_{vec}) = h_0(t) \exp(\beta^T F_{vec})$$

where F_{vec} represents the features extracted by the LSTM, with dimensions $N \times U$. The primary objective of model training is to maximize the partial likelihood function $L(\beta)$. After training, the model summary explains the impact of the features extracted by the LSTM on patient risk, including the value of the concordance index, the impact of features on the hazard ratio, and the statistical significance of the coefficients.

2.5.3. LIME inspection

To gain a deeper understanding of the LSTM model's contribution to predicting bladder cancer recurrence, this study employs the Local Interpretable Model-Agnostic Explanations (LIME) method. LIME provides detailed explanations of model predictions at the individual sample level, revealing the most influential features and their contributions[16]. Mathematically, LIME approximates the behavior of a complex model near a point using a local linear model, represented as $\xi(x) = \arg \min_{g \in G} L(f, g, \pi_x) + \Omega(g)$, where x is the sample point to be explained, f is the model in this study, g is the simple model (usually a linear model), G is the class of simple models, π_x is a weighting function defined near the sample x , L is the loss function between the predictions of the complex model and the simple model, and $\Omega(g)$ measures the complexity of the model.

First, a prediction function is defined to convert the test data into a format suitable for the LSTM model and make predictions, allowing the extraction of the output for specific samples from the model. Subsequently, an explainer capable of interpreting the predictions of the complex model is created. The training data, feature names, and regression mode are input to fit the prediction requirements of this study.

To analyze feature contributions, LIME analysis is performed for each test sample, generating corresponding feature contribution reports. These reports clarify the most important

features in the model's predictions and their contributions, helping us understand the model's behavior in specific situations. Python's Counter function is used to calculate the frequency of each feature's appearance in the LIME explanations. This not only reveals the most important features across all samples but also demonstrates their overall impact on model predictions.

2.5.4. Gradient Test Verification

To further analyze how the LSTM model processes input features at different time steps, a gradient test is conducted. This test aims to reveal the extent to which input features influence the output of the model's hidden layers, thereby understanding the feature sensitivity of the model at various time steps[17].

First, a gradient function G is defined to describe the influence of the input on the hidden state, mathematically expressed as $G(X_t, h_{t-1}; \theta) = \frac{\partial h_t}{\partial X_t}$, where X_t represents the input feature at time step t , h_{t-1} is the hidden state of the previous time step, h_t is the hidden state of the current time step, and θ represents the model parameters. The training data are converted into TensorFlow tensors, and these gradients are calculated through the forward propagation and automatic differentiation functions of the LSTM model.

Next, the average gradients of the input features at each time step for all samples are calculated, represented as $\bar{G}_{X_t} = \frac{1}{N} \sum_{i=1}^N G(X_t^{(i)}, h_{t-1}^{(i)}; \theta)$, where N is the total number of samples. By analyzing these average gradients, the study identifies the features that have the greatest impact on the model's predictions. Additionally, the frequency of each feature being identified as the maximum gradient feature is counted, providing data support for a quantitative assessment of the most critical features in the model's decision-making process.

2.5.5. t-SNE Visualization Analysis

To gain a deeper understanding of the intrinsic structure of features in the LSTM-Cox model and distinguish between different patient risk groups, this study utilizes the t-distributed Stochastic Neighbor Embedding (t-SNE) method for visualization analysis[18]. The t-SNE object implements a two-dimensional reduction of the training features, with the component parameters set to 2, a perplexity of 30, and 3000 iterations. This results in a two-dimensional feature space that reveals hidden information and clustering of samples. Using the matplotlib library, this analysis visualizes the clinical risk scores generated by the LSTM-Cox model. Patients are divided into high-risk and low-risk groups based on their risk scores, with each group clearly marked in different colors to visually distinguish risk levels in the feature space. This method not only explains how the model classifies patients according to risk but also visualizes the distribution of risk scores, providing a specific interpretation of the model's predictive capabilities and the feature space.

2.6. Comparison of Traditional Survival and Recurrence Models

To test the performance of the LSTM-Cox model introduced in this study, we conducted a series of comparative analyses

against several well-known and established statistical models in survival analysis. This comparison includes the standard Cox proportional hazards model, the Wei, Lin, and Weissfeld (WLW) model[19], the Andersen-Gill model, and the Prentice, Williams, and Peterson (PWP) model[20]. Using the `survival` package in RStudio, we accurately applied these models to the same bladder cancer dataset, consistently considering variables such as treatment type, number of tumors, and size. Model evaluation employed the Akaike Information Criterion (AIC) as a metric to quantitatively assess and compare each model’s predictive accuracy and goodness of fit. This approach helps the study determine the performance of the LSTM-Cox model relative to traditional survival and recurrence models.

2.7. Validation on Simulated Dataset

To further validate the LSTM-Cox model, this study used the `reda` package in RStudio to create a simulated dataset following a Weibull distribution[21]. This simulation generated 50 patient samples, each fitted based on the Weibull proportional hazards function. By comparing event occurrence times with observation end times, the dataset had a censoring rate of approximately 40%. The dataset included continuous and binary variables, as well as simulated survival times and event indicators, with continuous variables following a normal distribution, binary variables following a binomial distribution, and observation end times also normally distributed. Data preprocessing was performed using the `dplyr` package to optimize the dataset for survival analysis, implementing adjustments such as adding stop columns and organizing data by ID and time columns. To verify the realism of the simulated data, the Cox proportional hazards model from the `survival` package was used to assess the significance of survival variables, ensuring the dataset’s suitability for survival analysis. The final step of validation involved comparing the results of the LSTM-Cox model with the traditional Cox model, evaluating model fit through AIC to demonstrate the relative robustness and accuracy of the LSTM-Cox model in survival prediction.

2.8. Software and Tools

The computations for this study were performed using Python 3.8.18, with the IDE being PyCharm 2023.2.1 (Community Edition). Deep learning tasks were conducted using PyTorch 2.0.1, and statistical analyses were performed using R 4.3.2.

3. Results

In this study, after one hundred epochs, the LSTM-Cox model demonstrated significant improvements in performance metrics. The model’s loss value decreased from an initial 0.3957 to 0.2147, indicating a substantial enhancement in the model’s ability to accurately capture and interpret key features of the bladder cancer recurrence dataset. After the training phase, the LSTM-Cox model showed a loss of 0.0844 on the

test dataset, suggesting a very low error rate in predicting unseen data. Additionally, the model exhibited a concordance index of 0.90, a critical metric highlighting the accuracy and reliability of the model in survival prediction, thereby confirming the robustness of assumption 1.

The Cox test on the model revealed detailed information about the coefficients of each covariate and their statistical significance. Notably, the coefficient of the third covariate was 8.50 with a p-value less than 0.005, and the coefficient of the fifth covariate was -27.09, also with a p-value less than 0.005. These results not only underscore the significant impact of these covariates on the model’s predictions but also emphasize their statistical importance. These findings clearly indicate the decisive role of these covariates in the model’s predictions, and this role is statistically significant.

To explore the relationship between the clinical features extracted by the LSTM-Cox model and the original dataset features, the LIME results significantly revealed the contribution of features from the original dataset to the LSTM-Cox model’s predictions. An in-depth analysis of the test samples highlighted the importance of features 6 (stop), 9 (rsize), and 4 (recur) extracted by the neural network in the model’s predictions, underscoring their critical role in risk prediction.

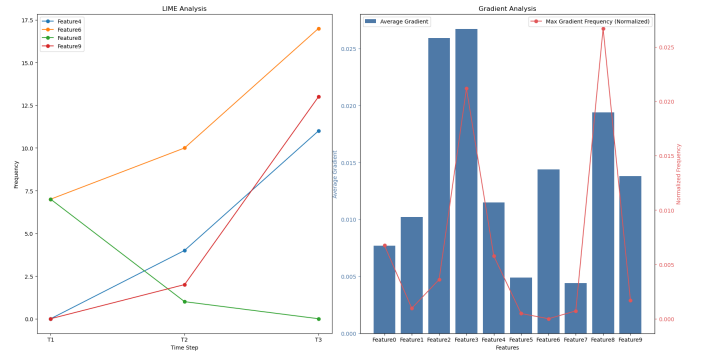


Figure 2: LIME and Gradient analysis displaying the frequency and impact of features on model predictions.

Additionally, by analyzing the frequency of all features in the LIME explanations, the study provides a comprehensive understanding of how each clinical feature of bladder cancer affects overall risk prediction. In this context, feature 6 was identified as the most important feature, appearing 51 times, followed by feature 9 (appearing 23 times) and feature 4 (appearing 22 times). Furthermore, feature 8 (rtumor) also appeared 13 times. The LIME test results emphasize the significant impact of specific features (especially 4, 6, 8, and 9) in the LSTM-Cox model, deepening our understanding of how the model’s decision-making process handles complex time-series data.

The gradient tests conducted on the LSTM model revealed the influence of different features on the model output. These tests showed that the variables "recur" and "rsize" have a significant impact on the model output, highlighting their importance. Statistical analysis of the gradient feature frequency further confirmed that "rsize" and "recur" are the main factors in-

fluencing the model’s predictions, underscoring the critical role of these variables in determining the clinical recurrence and survival outcomes of bladder cancer patients.

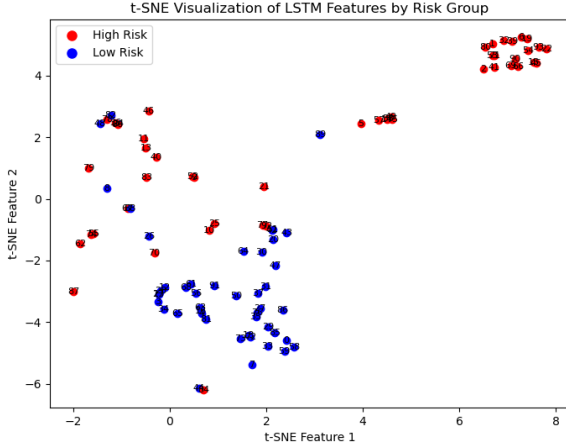


Figure 3: t-SNE visualization of LSTM features by risk group, illustrating the model’s ability to distinguish between different patient risk profiles.

t-SNE analysis helped visualize the features extracted by the LSTM model and clearly distinguish between high-risk and low-risk patient groups. The resulting plot shows the clustering of these two risk categories, with red and blue points representing high-risk and low-risk patients, respectively, highlighting how the model stratifies risk based on the learned features.

Table 3: Comparison of the LSTM-Cox model with traditional survival and recurrence models.

Model	Concordance index	AIC
LSTM-Cox	0.90	221.63
Cox	0.71	1829.34
WLW	0.78	-
Andersen-Gill	0.78	212.94
PWP	0.74	-

The LSTM-Cox model demonstrated outstanding performance on key metrics, particularly in predictive accuracy, as indicated by the concordance index, and model suitability, as reflected by the AIC, comprehensively outperforming traditional survival and recurrence models. The model’s high concordance index proves its reliability in assessing clinical recurrence risk, while the lower AIC value indicates its excellent predictive performance in handling model complexity.

Additionally, reliability analysis was performed on a simulated dataset constructed based on the Weibull distribution using the Cox proportional hazards model. The analysis results showed that the simulated dataset effectively replicated real-world clinical recurrence patterns and identified the variable X.1 as a significant predictor ($p=0.0049$), with a concordance index of 0.574. After verifying the applicability of the simulated dataset, this study further integrated the LSTM with the Cox proportional hazards model. On the same dataset, the

LSTM-Cox model outperformed traditional models, achieving a concordance index of 0.70 and an AIC value of 135.89, highlighting its reliability in predicting recurrence events and validating the effectiveness of model assumption 2. Furthermore, the model’s likelihood ratio test result was 19.20, with a significant p-value, further proving the statistical robustness and practical potential of the LSTM-Cox model. These results indicate that the proposed model has significant advantages in predictive accuracy and data fitting capability.

4. Discussion

In this study, the LSTM-Cox model demonstrated a significant improvement in predictive performance when handling the bladder cancer clinical recurrence dataset, exhibiting low prediction error and a high C-index of up to 0.90. These results not only prove the model’s efficiency in dealing with complex, time-dependent clinical data but also highlight its significant advantages in accuracy and efficiency compared to traditional methods. This advancement addresses the shortcomings of traditional methods mentioned in the introduction, showcasing the effective combination of LSTM’s time series analysis capability and the Cox model’s statistical analysis power. This provides a concise, powerful, and easy-to-apply deep learning strategy, which is highly valuable in the current research environment[22].

Specifically, by rigorously evaluating the LSTM-Cox model, including using LIME and gradient analysis, we elucidated the key operational mechanisms of the model in predicting clinical risk in the context of bladder cancer recurrence. The LIME evaluation particularly highlighted the significant impact of certain predictors, such as feature 6 (treatment stop time), feature 9 (maximum tumor size at recurrence), and feature 4 (recurrence frequency), which are crucial factors in the model’s risk prediction. The repeated identification of feature 6 emphasizes the critical role of treatment duration in predicting recurrence, while the significance of "rsize" and "recur" reveals their important contributions to risk prediction. The complementary results of the gradient analysis further emphasize the important influence of "treatment", "rsize", and "recur" on the model output. Specifically, the significance of "rsize" and "recur" in the gradient feature frequency analysis confirms these clinical features’ critical roles in assessing the recurrence risk of bladder cancer patients. These findings suggest that tumor size, recurrence frequency, and treatment type are key prognostic indicators in the treatment and recurrence stages of bladder cancer, aligning with the clinical trial results on bladder cancer recurrence discussed in the introduction. Through LIME evaluation and gradient analysis, the model has demonstrated its strong ability to identify and interpret key variables in the clinical recurrence dataset, enhancing its practicality and applicability and elevating its importance in clinical data analysis. Especially in handling recurrence event data, this model surpasses the limitations of traditional models in a concise and effective manner, bringing innovation to this complex field.

Additionally, we effectively visualized the features extracted by the LSTM model using the t-SNE method, showing a clear

distinction between high-risk and low-risk patient groups. This two-dimensional visualization method not only enhanced our understanding of the model's classification ability but also validated the effectiveness of the LSTM model in practical applications, particularly in identifying patients with different risk levels. The LSTM-Cox model's broad applicability and robustness were also confirmed by applying it to a simulated dataset constructed based on the Weibull distribution. This validation not only supports the theoretical effectiveness of the model but also provides a solid foundation for its potential application to a wider range of clinical recurrence datasets.

However, the model's applicability to other broader datasets needs further validation. Future research will focus on refining the model architecture, enhancing parameter validation to extend its application to various clinical recurrence datasets, and improving its interpretability for broader and more effective use in clinical settings[23][24].

In summary, the LSTM-Cox model presented in this study, statistically validated, shows significant advantages in efficiency and usability. By deeply exploring the contributions of key clinical predictors, it demonstrates practicality, applicability, and innovation. These characteristics make it a powerful tool for handling clinical recurrence data, providing profound insights into integrating advanced machine learning techniques with upcoming clinical decision support systems, heralding widespread applications in predicting and analyzing bladder cancer recurrence[25][26].

5. Conclusion

In this study, we designed and implemented the LSTM-Cox model, which demonstrated significant simplicity and efficiency in predicting clinical recurrence events such as bladder cancer. This model combines the predictive power of Long Short-Term Memory networks with the Cox proportional hazards model, significantly improving predictive accuracy, as indicated by a concordance index of up to 0.90. Its architecture not only overcomes the limitations of traditional methods but also simplifies the complexity of analyzing time-dependent data, enhancing ease of use for clinical practitioners. Future work will extend this model to more datasets and optimize its structure to improve performance and interpretability, enhancing its practical application in clinical settings. The LSTM-Cox model integrates complex deep learning techniques, showcasing the potential to enhance clinical outcomes through in-depth analysis of recurrence data, and aims to apply advanced analytical methods to clinical decision-making.

References

- [1] D. R. Cox, Regression models and life-tables, *Journal of the Royal Statistical Society: Series B (Methodological)* 34 (2) (1972) 187–202.
- [2] P. K. Andersen, R. D. Gill, Cox's regression model for counting processes: a large sample study, *The annals of statistics* (1982) 1100–1120.
- [3] J. L. Katzman, U. Shaham, A. Cloninger, J. Bates, T. Jiang, Y. Kluger, Deepsurv: personalized treatment recommender system using a cox proportional hazards deep neural network, *BMC medical research methodology* 18 (2018) 1–12.
- [4] E. Giunchiglia, A. Nemchenko, M. van der Schaar, Rnn-surv: A deep recurrent model for survival analysis, in: *Artificial Neural Networks and Machine Learning–ICANN 2018: 27th International Conference on Artificial Neural Networks, Rhodes, Greece, October 4–7, 2018, Proceedings, Part III* 27, Springer, 2018, pp. 23–32.
- [5] G. Gupta, V. Sunder, R. Prasad, G. Shroff, Cresa: a deep learning approach to competing risks, recurrent event survival analysis, in: *Advances in Knowledge Discovery and Data Mining: 23rd Pacific-Asia Conference, PAKDD 2019, Macau, China, April 14–17, 2019, Proceedings, Part II* 23, Springer, 2019, pp. 108–122.
- [6] S.-h. Jeong, J. H. Han, C. W. Jeong, H. H. Kim, C. Kwak, H. D. Yuk, J. H. Ku, Clinical determinants of recurrence in pta bladder cancer following transurethral resection of bladder tumor, *BMC cancer* 22 (1) (2022) 631.
- [7] A. Loras, M. Trasserra, D. Sanjuan-Herráez, M. Martínez-Bisbal, J. Castell, G. Quintás, J. Ruiz-Cerdá, Bladder cancer recurrence surveillance by urine metabolomics analysis, *Scientific reports* 8 (1) (2018) 9172.
- [8] J. Y.-C. Teoh, A. M. Kamat, P. C. Black, P. Grivas, S. F. Shariat, M. Babjuk, Recurrence mechanisms of non-muscle-invasive bladder cancer—a clinical perspective, *Nature Reviews Urology* 19 (5) (2022) 280–294.
- [9] A. T. Shalata, M. Shehata, E. Van Bogaert, K. M. Ali, A. Alksas, A. Mahmoud, E. M. El-Gendy, M. A. Mohamed, G. A. Giridharan, S. Contractor, et al., Predicting recurrence of non-muscle-invasive bladder cancer: current techniques and future trends, *Cancers* 14 (20) (2022) 5019.
- [10] O. Bratu, D. Marcu, R. Anghel, D. Spinu, L. Iorga, I. Balescu, N. Bacalbasa, C. Diaconu, C. Savu, C. Savu, et al., Tumoral markers in bladder cancer, *Experimental and therapeutic medicine* 22 (1) (2021) 1–8.
- [11] S. Hochreiter, J. Schmidhuber, Long short-term memory, *Neural computation* 9 (8) (1997) 1735–1780.
- [12] A. Graves, A.-r. Mohamed, G. Hinton, Speech recognition with deep recurrent neural networks, in: *2013 IEEE international conference on acoustics, speech and signal processing, Ieee*, 2013, pp. 6645–6649.
- [13] F. A. Gers, J. Schmidhuber, F. Cummins, Learning to forget: Continual prediction with lstm, *Neural computation* 12 (10) (2000) 2451–2471.
- [14] T. Hastie, R. Tibshirani, J. H. Friedman, J. H. Friedman, *The elements of statistical learning: data mining, inference, and prediction*, Vol. 2, Springer, 2009.
- [15] C. M. Bishop, *Pattern recognition and machine learning*, Springer google schola 2 (2006) 645–678.
- [16] M. T. Ribeiro, S. Singh, C. Guestrin, "why should i trust you?" explaining the predictions of any classifier, in: *Proceedings of the 22nd ACM SIGKDD international conference on knowledge discovery and data mining*, 2016, pp. 1135–1144.
- [17] M. Sundararajan, A. Taly, Q. Yan, Axiomatic attribution for deep networks, in: *International conference on machine learning*, PMLR, 2017, pp. 3319–3328.
- [18] M. Wattenberg, F. Viégas, I. Johnson, How to use t-sne effectively, *Distill* 1 (10) (2016) e2.
- [19] L.-J. Wei, D. Y. Lin, L. Weissfeld, Regression analysis of multivariate incomplete failure time data by modeling marginal distributions, *Journal of the American statistical association* 84 (408) (1989) 1065–1073.
- [20] R. L. Prentice, B. J. Williams, A. V. Peterson, On the regression analysis of multivariate failure time data, *Biometrika* 68 (2) (1981) 373–379.
- [21] W. Weibull, A statistical distribution function of wide applicability, *Journal of applied mechanics* (1951).
- [22] C. H. Lee, H.-J. Yoon, Medical big data: promise and challenges, *Kidney research and clinical practice* 36 (1) (2017) 3.
- [23] K. Batko, A. Ślęzak, The use of big data analytics in healthcare, *Journal of big Data* 9 (1) (2022) 3.
- [24] R. J. Chen, M. Y. Lu, J. Wang, D. F. Williamson, S. J. Rodig, N. I. Lindeman, F. Mahmood, Pathomic fusion: an integrated framework for fusing histopathology and genomic features for cancer diagnosis and prognosis, *IEEE Transactions on Medical Imaging* 41 (4) (2020) 757–770.
- [25] W. Liang, J. Yao, A. Chen, Q. Lv, M. Zanin, J. Liu, S. Wong, Y. Li, J. Lu, H. Liang, et al., Early triage of critically ill covid-19 patients using deep learning, *Nature communications* 11 (1) (2020) 3543.
- [26] Z. Obermeyer, E. J. Emanuel, Predicting the future—big data, machine learning, and clinical medicine, *The New England journal of medicine* 375 (13) (2016) 1216.